Quadrotor Attitude Control using Incremental Nonlinear Dynamics Inversion

Rodrigo Coelho[1], Alexandra Moutinho[2] and José Raul Azinheira[2]

[1]*Instituto Superior Técnico, Universidade de Lisboa, Portugal*
[2]*IDMEC, Instituto Superior Técnico, Universidade de Lisboa, Portugal*

Keywords: Incremental Nonlinear Dynamics Inversion, Quadrotor, Attitude Control, Sensor-based Control.

Abstract: Given the large flight envelope of vertical take-off and landing vehicles, and the nonlinear nature of multi-rotor aircraft, especially in aggressive maneuvering, nonlinear control strategies are often considered. Yet, most available solutions are model dependent and thus require a precise knowledge of the system dynamics, including the hard to model aerodynamics. This paper proposes a sensor-based approach to the problem. It considers a recent strategy based on incremental control and Nonlinear Dynamics Inversion (NDI), the Incremental Nonlinear Dynamics Inversion (INDI), to solve the attitude control problem of quadrotors. The INDI general formulation is presented, and then applied considering the attitude stabilization of a quadrotor. In order to apply the INDI solution to this case study, a linear predictor for the angular acceleration is provided. Simulation results demonstrate the robustness of this sensor-based approach to model-parameter uncertainties and wind disturbances. An analysis is also done regarding the tuning of INDI parameters and its sensitivity to the chosen sampling time.

1 INTRODUCTION

In these past few decades there has been a growing interest in unmanned aerial vehicles (UAVs). These vehicles are characterized by the absence of an on-board human pilot, being instead controlled remotely and/or by an onboard control system. This interest is brought by the recent technological advances in the area of microprocessors, microcontrollers and sensor systems as well as their respective manufacturing processes. Thanks to these advances the prices and sizes have been continuously decreasing and consequently UAVs have also become cheaper, smaller and easier to build. Their applications were initially reserved to the domain of military operations, where they decrease the risk of human loss and can increase efficiency, especially in tedious and/or dangerous missions such as covert or surveillance operations. Now UAVs are open to the general public and are being applied to new and different domains every day, such as aerial footage, fire prevention, search and rescue operations, monitoring of agriculture crops, infrastructure inspection and even multimedia or pure recreation.

There is a special interest in aircrafts with Vertical Take-Off and Landing (VTOL) capabilities due to their ability to operate with tighter spatial constraints than traditional fixed-wing aircraft. In this category the most studied aircraft are the helicopters and the multirotors where we have a need for robust and stable control as there is absence of dynamic pressure that in conventional aircraft is brought by the forward flight speed, ruling out inherent stability. Due to the unstable and nonlinear nature of multirotors and the large flight envelope associated to a VTOL, especially if aggressive maneuvering is necessary, nonlinear control strategies must be considered.

Several nonlinear solutions are presented for this problem such as Gain-Scheduling (Sadeghzadeh et al., 2011), Nonlinear Dynamics Inversion (NDI) (Mallikarjunan and et al., 2012), and Back-stepping (Mallikarjunan and et al., 2012), as well as adaptive (Krstic et al., 1995; Sadeghzadeh et al., 2011; Mallikarjunan and et al., 2012; Bastin, 2013) and robust (Liao et al., 2002; Goman and Kolesnikov, 1998) control techniques. However, these are approaches based on the knowledge of the system, and as such called model-based solutions. For the particular case of aircraft control, this model requirement can prove to be costly and time-consuming, as the aerodynamic coefficients, for example, require extensive wind-tunnel or flight tests to be properly identified.

Due to the general development of micro-electro-mechanical systems (MEMS), smaller, more accurate and more accessible sensors are available. This allows for sensor-based control approaches, where model knowledge is replaced by variable measurements. An example of these approaches is the Incremental Nonlinear Dynamics Inversion (INDI), an incremental variation of the Nonlinear Dynamics Inversion, and object of some recent studies regarding flight control (Sieberling et al., 2010; Simplício et al., 2013). It is relatively easy to design as it does not need the complete system model, only the input related part, because it uses sensor measurements to compensate for the state-only dependent dynamics such as the hard to model aerodynamics. This makes it more robust than traditional feedback linearization or NDI as it is not so sensitive to modeling errors. The downside are stricter requirements in the sampling frequency and the need for accurate sensors reading and/or variables estimation.

This paper addresses the INDI solution for the quadrotor attitude control problem. In order to better understand and evaluate this approach, the results presented test its robustness to model uncertainties and wind disturbances, as well as provide an insight on its sensitivity to design parameters.

The remaining of this paper is organized as follows. After the general formulation of INDI is introduced (sec. 2), and the model of the quadrotor is defined (sec. 3), the INDI control approach is applied to the quadrotor attitude control problem (sec. 4). Like for other feedback linearization approaches, this corresponds to the usual two-steps procedure of linearizing the system (here using INDI) and then applying linear control to the linearized system. The implementation requires that angular accelerations be available. In this paper they are estimated using a linear predictor. In section 5, a parameter tuning study regarding the INDI controller and the linear estimator is presented, followed by some simulation results that illustrate the solution performance and its robustness to model uncertainties and wind disturbances, as well as its sensitivity to the sampling time. Finally, section 7 closes with some final remarks.

2 NONLINEAR DYNAMICS INVERSION CONTROL THEORY

In order to better understand the incremental version of the nonlinear dynamics inversion, this section presents both classic and incremental formulations of this approach.

2.1 Nonlinear Dynamics Inversion

For the NDI formulation (Sieberling et al., 2010), consider the following affine n-th order MIMO system

$$\dot{\mathbf{x}} = \mathbf{f}(\mathbf{x}) + \mathbf{G}(\mathbf{x})\mathbf{u} \tag{1}$$

$$\mathbf{y} = \mathbf{h}(\mathbf{x}) \tag{2}$$

where $\mathbf{x} \in \mathbb{R}^n$ is the system state vector, $\mathbf{u} \in \mathbb{R}^m$ is the input vector, $\mathbf{f} \in \mathbb{R}^n$ and $\mathbf{h} \in \mathbb{R}^m$ are smooth vector fields, and $\mathbf{G} \in \mathbb{R}^{m \times n}$ is a matrix with each column $\mathbf{g}_i \in \mathbb{R}^n$ a smooth vector field.

By differentiating (2) with respect to time we have

$$\dot{\mathbf{y}} = \frac{d\mathbf{h}(\mathbf{x})}{dt} = \frac{\partial \mathbf{h}}{\partial \mathbf{x}}\dot{\mathbf{x}} \tag{3}$$

$$= \frac{\partial \mathbf{h}}{\partial \mathbf{x}}\mathbf{f}(\mathbf{x}) + \frac{\partial \mathbf{h}}{\partial \mathbf{x}}\mathbf{G}(\mathbf{x})\mathbf{u} \tag{4}$$

$$= L_\mathbf{f}\mathbf{h}(\mathbf{x}) + L_\mathbf{G}\mathbf{h}(\mathbf{x})\mathbf{u} \tag{5}$$

where $L_\mathbf{f}\mathbf{h}(\mathbf{x})$ and $L_\mathbf{G}\mathbf{h}(\mathbf{x})$ are the respective Lie Derivatives of $\mathbf{h}(\mathbf{x})$ with respect to $\mathbf{f}$ and $\mathbf{G}$. Assuming $L_\mathbf{G}\mathbf{h}(\mathbf{x})$ is invertible, the control action $\mathbf{u}$ may be isolated as:

$$\mathbf{u} = (L_\mathbf{G}\mathbf{h}(\mathbf{x}))^{-1}(\dot{\mathbf{y}} - L_\mathbf{f}\mathbf{h}(\mathbf{x})) \tag{6}$$

For $\mathbf{y} = \mathbf{x}$ and $\dot{\mathbf{y}}$ a desired system dynamics $\dot{\mathbf{x}}_d$, we have $L_\mathbf{G}\mathbf{h}(\mathbf{x}) = \mathbf{G}(\mathbf{x})$ and $L_\mathbf{f}\mathbf{h}(\mathbf{x}) = \mathbf{f}(\mathbf{x})$ and we can rewrite (6) as

$$\mathbf{u} = (\mathbf{G}(\mathbf{x}))^{-1}(\dot{\mathbf{x}}_d - \mathbf{f}(\mathbf{x})) \tag{7}$$

This produces a linearized system in the form $\dot{\mathbf{x}} = \dot{\mathbf{x}}_d$.

2.2 Incremental Nonlinear Dynamics Inversion

Opposed to NDI, INDI has no requirements for the input dynamics, so we can use a more generic formulation (Azinheira et al., 2015) for nonlinear systems such as

$$\dot{\mathbf{x}} = \mathbf{f}(\mathbf{x}, \mathbf{u}) \tag{8}$$

If we linearize (8) around the previous time step condition $(\mathbf{x}_0, \mathbf{u}_0)$ with $t_0 = t - T_s$ and T_s being the controller sampling time, we have

$$\dot{\mathbf{x}} \cong \dot{\mathbf{x}}_0 + \frac{\partial \mathbf{f}}{\partial \mathbf{x}}\Big|_{\mathbf{x}_0,\mathbf{u}_0}(\mathbf{x} - \mathbf{x}_0) + \frac{\partial \mathbf{f}}{\partial \mathbf{u}}\Big|_{\mathbf{x}_0,\mathbf{u}_0}(\mathbf{u} - \mathbf{u}_0) \tag{9}$$

where $\dot{\mathbf{x}}_0 = \mathbf{f}(\mathbf{x}_0, \mathbf{u}_0)$. Assuming a small enough sampling time T_s, the state variation between samples can be considered negligible ($\mathbf{x} \approx \mathbf{x}_0$). We can then simplify (9) as

$$\dot{\mathbf{x}} \approx \dot{\mathbf{x}}_0 + \frac{\partial \mathbf{f}}{\partial \mathbf{u}}\Big|_{\mathbf{x}_0,\mathbf{u}_0}(\mathbf{u} - \mathbf{u}_0) \tag{10}$$
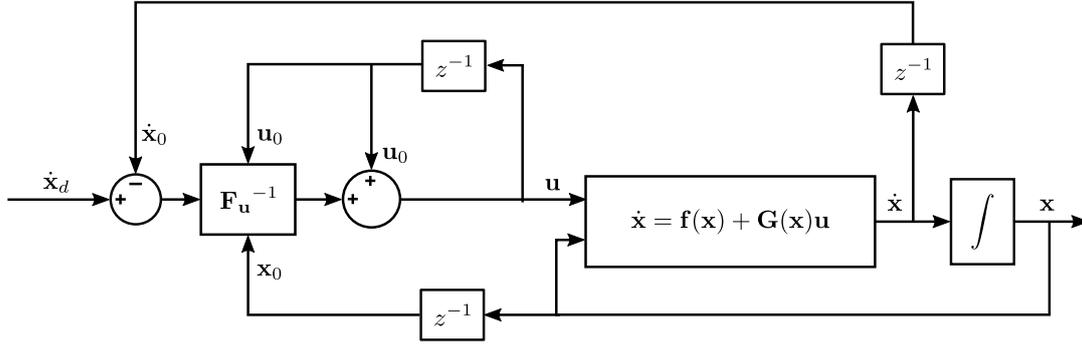
Figure 1: Block diagram representation of INDI control scheme.

Setting the desired dynamics as $\dot{\mathbf{x}} = \dot{\mathbf{x}}_d$ and defining $\mathbf{F}_u = \frac{\partial \mathbf{f}}{\partial \mathbf{u}}\big|_{\mathbf{x}_0, \mathbf{u}_0}$ we obtain the following control input

$$\mathbf{u} = \mathbf{u}_0 + \mathbf{F}_u^{-1}(\dot{\mathbf{x}}_d - \dot{\mathbf{x}}_0) \qquad (11)$$

where $\mathbf{F}_u$ must be invertible and $\dot{\mathbf{x}}_0$, $\mathbf{x}_0$ and $\mathbf{u}_0$ must be available.

The INDI control scheme is described by the block diagram of figure 1.

3 QUADROTOR MODEL

This section presents the quadrotor nonlinear model. In order to do so, the required reference frames are first introduced, followed by the kinematic and dynamic equations of motion.

3.1 Reference Frames

The first spatial reference necessary is the inertial frame, a frame that describes time and space homogeneously, isotropically, and in a time-independent manner. We assume the "flat Earth" model and use a North-East-Down (NED) frame located in the surface of the Earth and centered on the quadrotor initial position, $I = (O_I; x_I; y_I; z_I)$, as the inertial reference frame. We will also define a frame fixed to the quadrotor and centered in its center of gravity, $\mathcal{B} = (O_{\mathcal{B}}; x_{\mathcal{B}}; y_{\mathcal{B}}; z_{\mathcal{B}})$, as seen in figure 2.

Another frame that needs to be defined is the Inertial Measurement Unit (IMU) frame. This frame is centered in the IMU at $d_{\text{IMU}} = (x_{\text{IMU}}, y_{\text{IMU}}, z_{\text{IMU}})$ relative to the $\mathcal{B}$ frame and also fixed to the quadrotor.

3.2 Kinematics

The kinematics describes the movement of the quadrotor in the inertial frame I. To describe the position $\mathbf{P}$ of the quadrotor in I frame we can consider
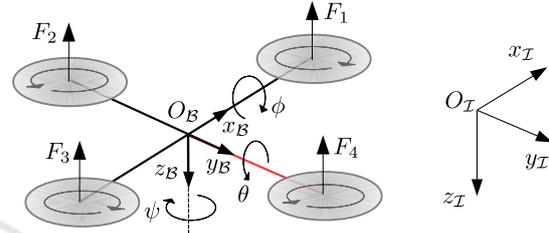
Figure 2: Inertial and body-centered coordinate systems (Esteves et al., 2015).

the following transformation

$$\dot{\mathbf{P}} = \mathbf{R}^T \mathbf{V} \qquad (12)$$

where $\mathbf{P} = (x, y, z)^T$ is the body position in I frame, $\mathbf{V} = (u, v, w)^T$ is the linear velocity in $\mathcal{B}$ frame and $\mathbf{R}$ is the rotation matrix from I to $\mathcal{B}$ frames expressed using the quadrotor attitude represented using quaternions $\mathbf{Q} = (q_0, q_1, q_2, q_3)^T$

$\mathbf{R} =$

$$\begin{bmatrix} 1 - 2q_2^2 - 2q_3^2 & 2(q_1 q_2 + q_3 q_0) & 2(q_1 q_3 - q_2 q_0) \\ 2(q_1 q_2 - q_3 q_0) & 1 - 2q_1^2 - 2q_3^3 & 2(q_2 q_3 + q_1 q_0) \\ 2(q_1 q_3 + q_2 q_0) & 2(q_2 q_3 - q_1 q_0) & 1 - 2q_1^3 - 2q_2^2 \end{bmatrix}$$
$$(13)$$

The rotational kinematics is described by

$$\dot{\mathbf{Q}} = \mathbf{S}_Q \boldsymbol{\omega} \qquad (14)$$

where $\boldsymbol{\omega} = (p, q, r)^T$ is the angular velocity of the quadrotor in the three main directions of $\mathcal{B}$ frame and $\mathbf{S}_Q$ is a transformation matrix that using the quaternions attitude representation is defined as

$$\mathbf{S}_Q = -\frac{1}{2} \begin{bmatrix} q_1 & q_2 & q_3 \\ -q_0 & q_3 & -q_2 \\ -q_3 & -q_0 & q_1 \\ q_2 & -q_1 & -q_0 \end{bmatrix} \qquad (15)$$

3.3 Dynamics

The dynamics model used is based on Newton-Euler approach following (Stevens and Lewis, 2003).

The translational dynamics is given by

$$m\dot{\mathbf{V}} = \mathbf{F}_P + \mathbf{F}_d + m\mathbf{Rg} - m\mathbf{\Omega V} \qquad (16)$$

with $\mathbf{F}_P = (0, 0, \sum_{j=1}^{4} F_j)^T$ the generalized rotors force where F_j, $j = 1, 2, 3, 4$ is the force produced by rotor j, $\mathbf{F}_d \in \mathbb{R}^3$ the aerodynamics drag force and $m\mathbf{Rg} = \mathbf{F}_g \in \mathbb{R}^3$ the gravitational force expressed in $\mathcal{B}$ frame. The cross-product matrix $\mathbf{\Omega} = \boldsymbol{\omega} \times \in \mathbb{R}^{3 \times 3}$ associated with the Coriols term $m\mathbf{\Omega V}$ is defined as

$$\mathbf{\Omega} = \begin{bmatrix} 0 & -r & q \\ r & 0 & -p \\ -q & p & 0 \end{bmatrix} \qquad (17)$$

The rotational dynamics is described by

$$\mathbf{J}\dot{\boldsymbol{\omega}} = -\mathbf{\Omega J \boldsymbol{\omega}} + \boldsymbol{\tau}_P \qquad (18)$$

with $\mathbf{\Omega J \boldsymbol{\omega}}$ the Coriolis torque related term, $\boldsymbol{\tau}_P = \left(r_m(F_2 - F_4),\ r_m(F_1 - F_3),\ \sum_{j=1}^{4} (-1)^{j+1} \tau_j \right)^T$ the rotors generalized torque where F_j, τ_j, $j = 1, 2, 3, 4$ are the force and torque produced by rotor j, r_m is the distance between the rotors and the quadrotor center of mass, and where the aerodynamic drag torque $\boldsymbol{\tau}_D \in \mathbb{R}^3$ was neglected given the quadrotor reduced dimensions.

4 APPLICATION TO QUADROTOR ATTITUDE CONTROL

This section concerns the INDI application to the quadrotor attitude control. Being a feedback linearization methodology, the control design corresponds to the usual two-steps procedure of linearizing the system (here using NDI or INDI for comparison) and then applying linear control to the linearized system. The implementation also requires that angular accelerations be available, and with that purpose a linear predictor is introduced. The complete solution is depicted in the block diagram of fig. 3.

4.1 System Linearization

In order to provide a better comparison between classic and incremental nonlinear dynamics inversion approaches, both formulations will be applied to the quadrotor attitude control problem. Both formulations consider $\mathbf{x} = [\boldsymbol{\omega}^T, \mathbf{Q}^T]^T$, $\mathbf{u} = \boldsymbol{\tau}_p$ and $\mathbf{y} = \mathbf{x}$.

4.1.1 NDI

For NDI we define $\mathbf{f}(\mathbf{x})$ and $\mathbf{G}(\mathbf{x})$ as

$$\mathbf{f}(\mathbf{x}) = \begin{bmatrix} -\mathbf{J}^{-1}\mathbf{\Omega J \boldsymbol{\omega}} \\ \mathbf{S}_Q \boldsymbol{\omega} \end{bmatrix} \qquad (19)$$

$$\mathbf{G}(\mathbf{x}) = \begin{bmatrix} \mathbf{J}^{-1} \\ \mathbf{0}_{4 \times 3} \end{bmatrix} \qquad (20)$$

Substituting (19)-(20) into (7) we obtain

$$\mathbf{u} = \begin{bmatrix} \mathbf{J}^{-1} \\ \mathbf{0}_{4 \times 3} \end{bmatrix}^+ \left(\begin{bmatrix} \dot{\boldsymbol{\omega}}_d \\ \dot{\mathbf{Q}}_d \end{bmatrix} - \begin{bmatrix} -\mathbf{J}^{-1}\mathbf{\Omega J \boldsymbol{\omega}} \\ \mathbf{S}_Q \boldsymbol{\omega} \end{bmatrix} \right) \qquad (21)$$

where $[\cdot]^+$ corresponds to the pseudo-inverse operation, and which simplified results in the NDI control law

$$\mathbf{u} = \mathbf{J}(\dot{\boldsymbol{\omega}}_d + \mathbf{J}^{-1}\mathbf{\Omega J \boldsymbol{\omega}}) \qquad (22)$$

where $\dot{\boldsymbol{\omega}}_d \in \mathbb{R}^3$ is a desired angular rate dynamics (acceleration).

4.1.2 INDI

For INDI we define $\mathbf{f}(\mathbf{x}, \mathbf{u})$ as

$$\mathbf{f}(\mathbf{x}, \mathbf{u}) = \begin{bmatrix} -\mathbf{J}^{-1}\mathbf{\Omega J \boldsymbol{\omega}} + \mathbf{J}^{-1}\boldsymbol{\tau} \\ \mathbf{S}_Q \boldsymbol{\omega} \end{bmatrix} \qquad (23)$$

and the derivative

$$\left. \frac{\partial \mathbf{f}}{\partial \mathbf{u}} \right|_{\mathbf{x}_0, \mathbf{u}_0} = \begin{bmatrix} \mathbf{J}^{-1} \\ \mathbf{0}_{4 \times 3} \end{bmatrix} \qquad (24)$$

Subsituting (23)-(24) into (11) we obtain

$$\mathbf{u} = \mathbf{u}_0 + \begin{bmatrix} \mathbf{J}^{-1} \\ \mathbf{0}_{4 \times 3} \end{bmatrix}^+ \left(\begin{bmatrix} \dot{\boldsymbol{\omega}}_d \\ \dot{\mathbf{Q}}_d \end{bmatrix} - \begin{bmatrix} \dot{\boldsymbol{\omega}}_0 \\ \dot{\mathbf{Q}}_0 \end{bmatrix} \right) \qquad (25)$$

that simplifies into the INDI control law

$$\mathbf{u} = \mathbf{u}_0 + \mathbf{J}(\dot{\boldsymbol{\omega}}_d - \dot{\boldsymbol{\omega}}_0) \qquad (26)$$

where $\dot{\boldsymbol{\omega}}_d \in \mathbb{R}^3$ and $\dot{\mathbf{Q}}_d \in \mathbb{R}^4$ are respectively desired angular rate and attitude dynamics and $\dot{\boldsymbol{\omega}}_0 \in \mathbb{R}^3$ and $\dot{\mathbf{Q}}_0 \in \mathbb{R}^4$ the last observed values of these variables.

Since this paper only addresses the attitude control, the vertical control is assumed to be dealt with by another control loop, which defines the value of the generalized forces $\mathbf{F}_P = (0, 0, \sum_{j=1}^{4} F_j)^T$, with F_j the thrust force produced by rotor j, and therefore the necessary thrust to keep the quadrotor hovering.

The control action defined by the NDI or INDI controllers corresponds to the generalized moments applied to the quadrotor by the four rotors, $\mathbf{u} = \boldsymbol{\tau}_p$. In order to apply the required control action, these generalized moments need to be converted into the four rotors angular speeds ω_{p_i}. This transformation is called control allocation and corresponds in this case to

$$\boldsymbol{\omega}_p = \sqrt{\mathbf{G}_a^+ \mathbf{u}} \qquad (27)$$
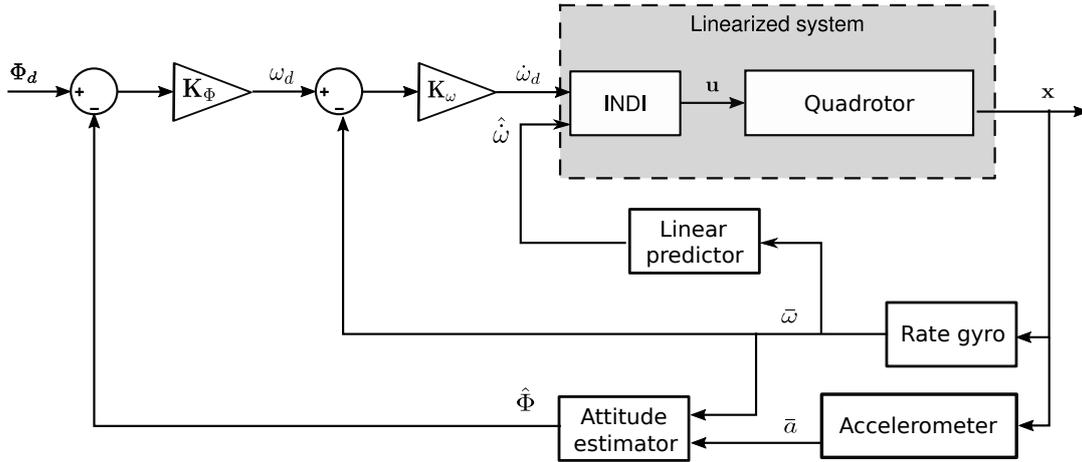
Figure 3: Block diagram representation of proposed attitude control solution.

where $\boldsymbol{\omega_p} = (\omega_1, \omega_2, \omega_3, \omega_4)^T$ are the rotors always positive angular speed and

$$\mathbf{G}_a = \begin{bmatrix} 0 & r_m K_{F_2} & 0 & -r_m K_{F_4} \\ r_m K_{F_1} & 0 & -r_m K_{F_3} & 0 \\ K_{\tau_1} & -K_{\tau_2} & K_{\tau_3} & -K_{\tau_4} \end{bmatrix} \quad (28)$$

with K_{τ_i}, $i = 1, 2, 3, 4$ the rotors torque coefficients.

4.2 Linear Control

Applying the NDI and INDI to the quadrotor model solves the problem of compensating the nonlinearities in the system. It does not, however, solve the complete attitude control problem. After the system linearization done by INDI (or NDI), we may now use linear control to stabilize each system state separately. We will use the principle of time scale separation to control the quadrotor attitude in two loops: an inner one that stabilizes the attitude rate $\boldsymbol{\omega}$ and an outer loop to control the attitude $\boldsymbol{\Phi}$ itself.

For each loop we consider a simple proportional controller

$$\dot{\boldsymbol{\omega}}_d = \mathbf{K}_\omega(\boldsymbol{\omega}_d - \boldsymbol{\omega}) \quad (29)$$

$$\boldsymbol{\omega}_d = \mathbf{K}_\Phi(\boldsymbol{\Phi}_d - \boldsymbol{\Phi}) \quad (30)$$

where the gains $\mathbf{K}_\omega \in \mathbb{R}^{3 \times 3}$ and $\mathbf{K}_\Phi \in \mathbb{R}^{3 \times 3}$ are diagonal matrices.

With the INDI linearization of the quadrotor dynamics, followed by the cascaded linear control, the closed-loop system can be represented as a second degree linear time-invariant system for each angle Φ_i, $i = 1, 2, 3$ as

$$\frac{\Phi_i}{\Phi_{i_d}} = \frac{K_{\omega_i} K_{\Phi_i}}{s^2 + K_{\omega_i} s + K_{\omega_i} K_{\Phi_i}} \quad (31)$$

where K_{ω_i} and K_{Φ_i} can be chosen according to our target damping coefficient ξ_i and natural frequency ω_{n_i}

as

$$K_{\omega_i} = 2\xi_i \omega_{n_i} \quad (32)$$

$$K_{\Phi_i} = \frac{\omega_{n_i}}{2\xi_i} \quad (33)$$

These two parameters need to be chosen so that the controlled system follows the performance requirements. We follow (Esteves et al., 2015) and choose the following performance requirements for the attitude response

- A 4.3% overshoot allowed;

- For roll and pitch, a rising time inferior to 1 second and a settling time inferior to 3 seconds for a step reference;

- For yaw, a rising time inferior to 4 sec and a settling time inferior to 8 seconds for a step reference.

The parameters chosen are presented in table 1 and the step response of the linearized system is presented in figure 4.

Table 1: Linear controller gains.

Angle	ξ	ω_n (rad/s)	$\mathbf{K}_{\omega_i}$	$\mathbf{K}_{\Phi_i}$
roll (ϕ)	0.79	6.32	10	4
pitch (θ)	0.79	6.32	10	4
yaw (ψ)	0.9	1.5	2.7	0.83

4.3 Linear Predictor for Angular Acceleration Estimation

To implement the INDI controller, precise information about the quadrotor angular acceleration $\dot{\boldsymbol{\omega}}$ is
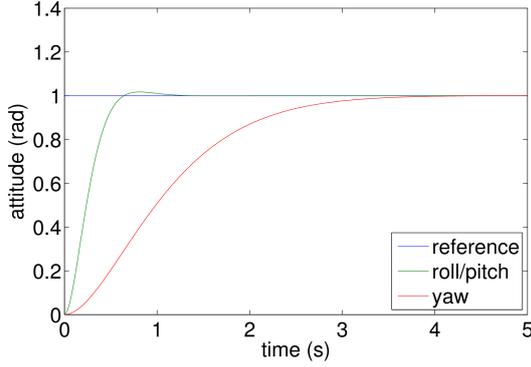
Figure 4: Step response of the attitude closed-loop system.

needed. This information is not directly obtained from sensor measurements, so an estimator is required. Following (Sieberling et al., 2010), we present a linear predictor that takes advantage of the INDI controller characteristics to solve the problem of delay in real-world sensors. As the INDI controller decouples the quadrotor dynamics and the linear control outer loops define each linearized state response, we can design a decoupled linear estimator for each state. The estimator structure is

$$\dot{\boldsymbol{\omega}}_k = \sum_{i=1}^{5} [\boldsymbol{\theta}_{\omega,i}\boldsymbol{\omega}_{k-i} + \boldsymbol{\theta}_{d,i}\boldsymbol{\omega}_{d,k-i}] + \boldsymbol{\varepsilon} \qquad (34)$$

with $\boldsymbol{\omega}_{d,k-i}$ the desired angular speed given by the speed control loop, $\boldsymbol{\theta}_{\omega,i}$ and $\boldsymbol{\theta}_{d,i}$ the measured and desired angular speeds coefficients, and $\boldsymbol{\varepsilon}$ white noise.

To calculate the estimator coefficients we use the least-squares method with simulation data of a linear system that represents the quadrotor behavior when linearized with INDI and controlled by a decoupled linear regulator. The SISO transfer function is

$$\frac{\omega(s)}{\omega_r(s)} = \frac{K}{s+K} \qquad (35)$$

with $\omega(s)$ the angular speed, $\omega_d(s)$ the desired angular speed, and K the gain imposed by the angular rate inner control loop. The angular acceleration $\dot{\omega}$ is obtained by differentiation.

With the knowledge of the angular rate $\boldsymbol{\omega}$, the respective reference $\boldsymbol{\omega}_d$ and the angular acceleration $\dot{\boldsymbol{\omega}}$, the coefficients $\boldsymbol{\theta} = [\boldsymbol{\theta}_d \quad \boldsymbol{\theta}_{\dot{\omega}}]$ were estimated implementing the least-squares method in Matlab® along with a simulation of (35). The simulation run for 10 s considering a pulse reference with a $\pi/6$ rad height and 4 s duration, along with the system's response for the gains used in each angular rate control loop.

With the system's response $\boldsymbol{\omega}$ and the angular acceleration $\dot{\boldsymbol{\omega}}$ calculated by numeric differentiation, we solve

$$\boldsymbol{\theta} = (\mathbf{H}^T\mathbf{H})^{-1}\mathbf{H}^T\mathbf{z} \qquad (36)$$

where $\mathbf{H} = [1 \quad r^j_{(t-1dt)}...r^j_{(t-5dt)} \quad \omega^j_{(t-1dt)}...\omega^j_{(t-5dt)}]$ is known as the design matrix that contains the references r^j and angular rates ω^j in the last 5 samples and $\mathbf{z}$ is the vector that contains the angular accelerations one step ahead. Each row of matrix $\mathbf{H}$ and vector $\mathbf{z}$ represent each sample taken from the simulation at a frequency equal to the controller sampling frequency $1/T_s$.

5 SIMULATION RESULTS

This section presents the results and tests obtained in a Matlab/Simulink® implementation. We first explore the controller and estimator parameter tuning, and after evaluate the overall approach performance, namely its robustness to model uncertainties and its sensitivity to sampling time.

5.1 Design Parameter Tuning

5.1.1 INDI Controller

Following (Azinheira et al., 2015), the INDI controller implementation considers an additional control parameter η. This parameter weights the update of the control action $\Delta\mathbf{u} = \mathbf{F}_u^{-1}(\dot{\mathbf{x}}_d - \dot{\mathbf{x}}_0)$ in relation to the last input provided $\mathbf{u}_0$

$$\mathbf{u} = \mathbf{u}_0 + \eta\Delta\mathbf{u} \qquad (37)$$

Taking into account the integrative characteristic of INDI, we can compare η to an integral gain in a PID controller. Whereas in a PID controller the integral gain is meant to correct stationary errors, in INDI η is meant to dampen the integration to help cope with the imperfections in the actuation system and reduce the error amplification.

Figure 5 shows the required control action (angular speed for each motor ω_{p_i}) and the respective response of the system in roll angle ϕ to a step reference $\phi_d = 15$ deg for different values of the parameter η. We can see for the case of $\eta = 1$, equivalent to the theoretical INDI, that the required control action presents high frequency and amplitude oscillation that even hits the input saturation point at $\omega_{p_i} \approx 680$ rad/s. The attitude response (output) follows the reference ϕ_d similarly to the (linear) response ϕ_l of a theoretical second-order LTI system with the same damping coefficient and natural frequency as the linear control loop implemented, with some high-frequency but low amplitude oscillations. This low amplitude of the oscillations is due to the inherent damping of higher-frequencies of the quadrotor dynamics. As we lower

(a) η = 1

(b) η = 0.9

(c) η = 0.3

(d) η = 0.1
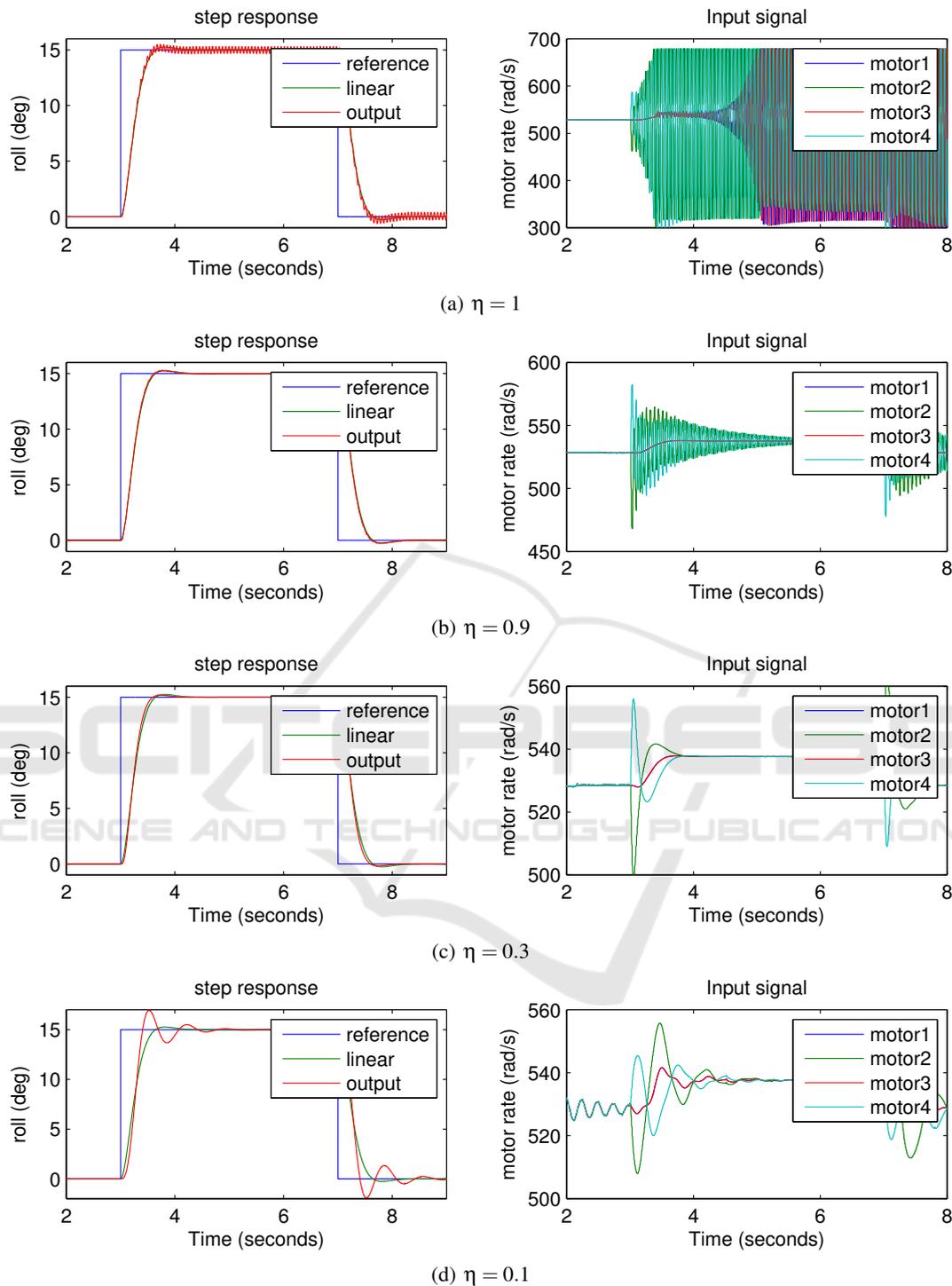
Figure 5: Step response and INDI required control action for different η.

the value of η we can observe a decrease in the required control action ω_{p_i} and respective oscillations. When η is lowered to 0.1, the required control action oscillations increase again though with lower frequency. A clear deterioration of the attitude response is observed, with an increase of the overshoot as well as of the settling time, probably consequence of the response to errors becoming too slow with the accentuated decrease in the INDI integration. Making a balance between required control action, response time

and oscillation damping, we set $\eta = 0.3$.

5.1.2 Angular Acceleration Estimation

A frequent problem in estimation is the delay in measurements. Besides the measurements accuracy, it is important to minimize measurement delay since it may seriously deteriorate the performance of the controlled system. Additional to these issues, in the case of our controlled system we observed a different phenomena, as the linear predictor assumes a linear system response and gives a very small weight to the actual measurements. This results in a response estimation which is faster than the real system response, as presented in figure 6. This happens because when adding the η parameter to the INDI implementation, the resulting linearization is no longer pure, resulting on a slower response. Closing the loop, we verify that this slower response leads to a desynchronization between the estimated angular acceleration and the real one. As the estimation is faster than the true acceleration, we experimented adding a delay to the estimator. Figure 7 presents the estimated angular acceleration $\hat{\dot{\boldsymbol{\omega}}}$ for different delay values b, for both open- and closed-loop scenarios. We can observe that increasing the estimation delay to $b = 2$ increases the synchronization of the closed-loop response and decreases oscillation. A higher delay results in a response oscillation increase. The estimation error is still significant and further improvement in the estimation should improve the closed-loop response.

5.2 Robustness to Model Uncertainties

In order to evaluate the performance of the proposed sensor-based solution, we will evaluate its robustness to model uncertainties. In the quadrotor control case, we will test the only model element that is explicit in the INDI control law, the matrix of inertia. To represent the model inaccuracies we will multiply the real inertia matrix $\mathbf{J}$ (used in the quadrotor dynamics simulator) by a factor σ representing the parameter uncertainty. The estimated inertia $\tilde{\mathbf{J}}$

$$\tilde{\mathbf{J}} = \sigma \mathbf{J} \tag{38}$$

is the inertia used by the INDI control law.

Assuming perfect sensors, figure 8 shows the response of the controlled system to a step reference in roll angle. Figure 8(a) presents the system response when INDI assumes an inertia lower than the real one. We can observe that for $\sigma = 0.4$ (in fact for $0.4 \leq \sigma < 1$) the controlled system has a response very close to the nominal one ($\sigma = 1$). When $\sigma = 0.3$, the controlled system response shows high frequency oscillations and for lower values ($\sigma < 0.3$) the system

becomes unstable. Figure 8(b) shows that the system response for $\sigma \leq 2$ is a little more oscillatory, corresponding to a slightly faster response. For $\sigma \geq 3$ we have a higher overshoot and settling time, which for higher values of σ may result in the system instability. This means that even with an underestimation of 60% or overestimation of 100% of the quadrotor inertia, the INDI controller still shows very little loss of performance.

Assuming real sensors and including the angular acceleration estimation, figure 9 presents the controlled quadrotor response to a 15 deg reference step in roll angle for different values of σ. We can observe an evolution similar to the perfect sensors test, with the controlled response degraded with the higher variation of the inertia uncertainty. This degradation happens for smaller inertia errors as we can see in fig. 9(a) for inertia underestimation and on fig. 9(b) for inertia overestimation. For this more realistic scenario, we observe that the controlled system performance is similar for $0.5 \leq \sigma \leq 1.5$, corresponding to a smaller but still significant robustness to model uncertainty.

5.3 Sensitivity to Sampling Time

The deduction of the INDI control law lies on the assumption that for a small enough sampling time the state variation between samples is negligible when compared to the actuation input. The satisfaction of this assumption requires in practice that the controller dynamics be much faster than the quadrotor dynamics. In the following we will check if this holds for our INDI controller implementation, and how high does this sampling rate need to be so that INDI is effective.

Figure 10 represents the system response to a 15 deg step in roll, where the chosen base sampling frequency $f_s = 100$ Hz is limited by the used sensors set. We can observe that the decrease of the sampling frequency below 50 Hz deteriorates the system response, presenting a higher overshoot and settling time. At $f_s = 20$ Hz the system seems close to stability limits and for lower sampling frequencies the system becomes unstable. These results show that, as expected, INDI is sensitive to the controller sampling frequency.

6 ROBUSTNESS TO WIND DISTURBANCES

One of the major advantages of INDI is its robustness to state-only dependent model uncertainties. In aircraft flight control this is an important characteristic as the most difficult to identify aerodynamic model
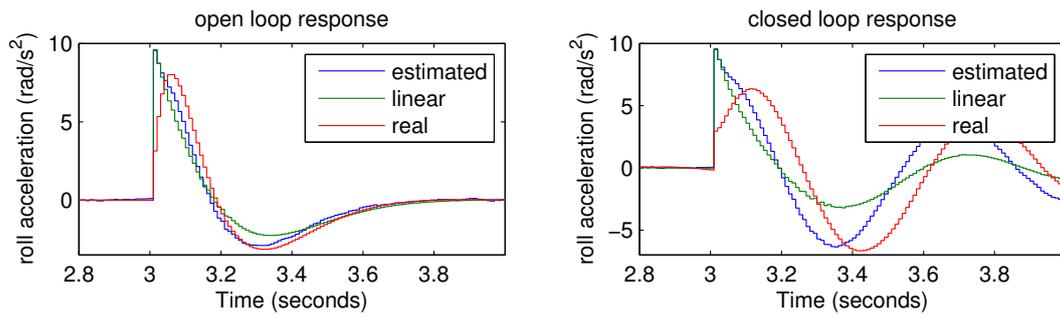
Figure 6: Angular acceleration estimation output.
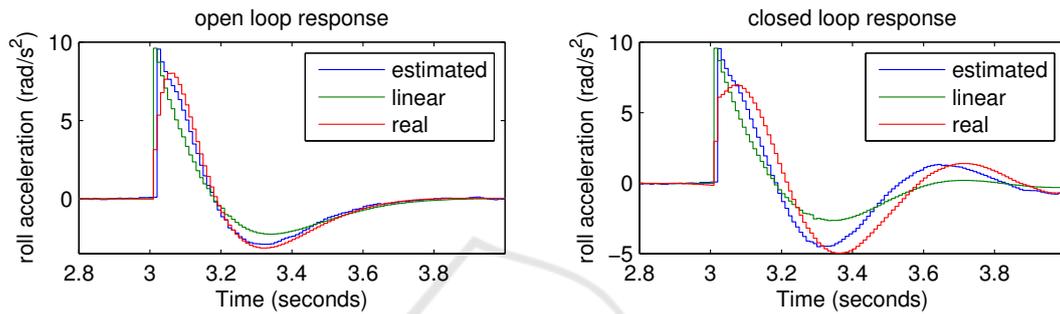
(a) $b = 1$
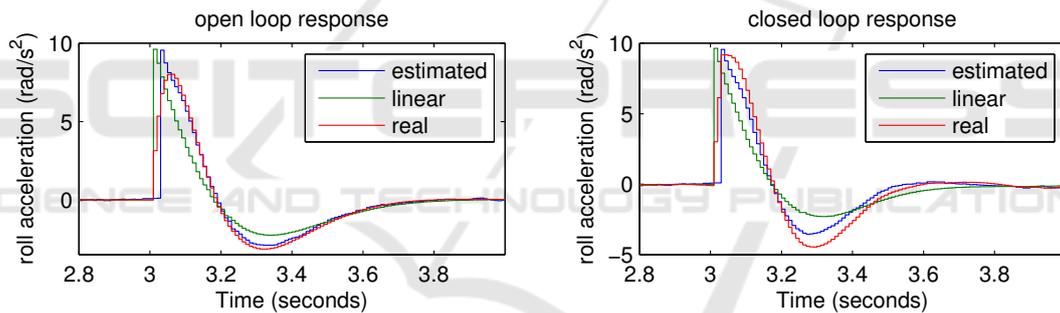
(b) $b = 2$
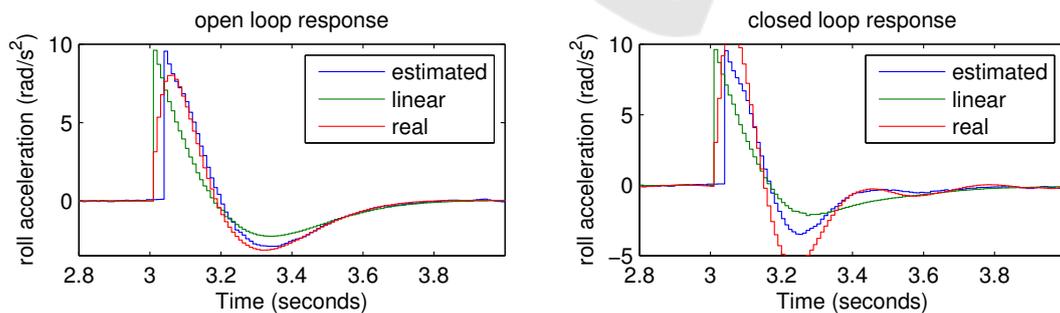
(c) $b = 3$

Figure 7: Estimation output with delay α.

part is grouped with the state-only dependent dynamics, usually requiring extensive work, such as wind tunnel tests or numeric fluid dynamic simulations. This is what makes the INDI control algorithm an attractive choice for flight control architectures, as it only requires the modelling and identification of the aerodynamics actuation part. This section demonstrates the INDI robustness to wind disturbances (for better results visualization, we only present the results with constant wind).
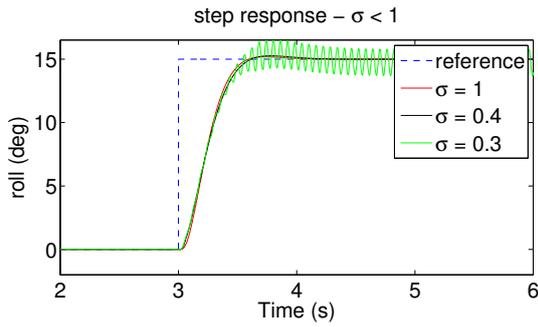
(a) $\sigma < 1$
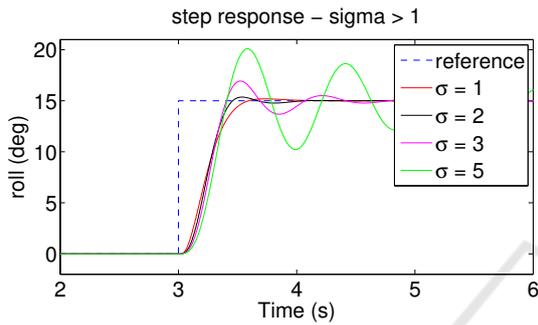
(b) $\sigma > 1$

Figure 8: Robustness to inertia uncertainty - results assuming perfect sensors.
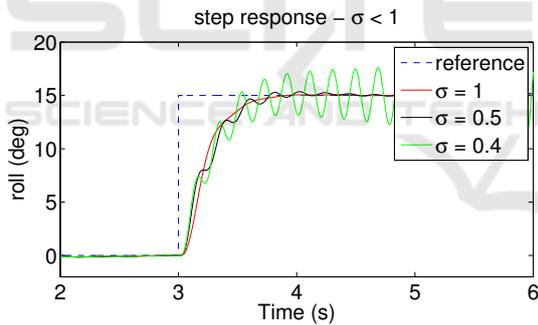
(a) $\sigma < 1$
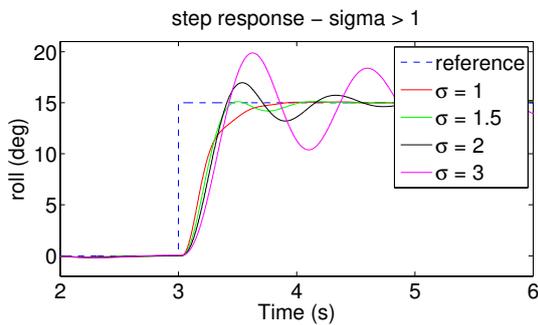
(b) $\sigma > 1$

Figure 9: Robustness to inertia uncertainty - results with angular acceleration estimation.
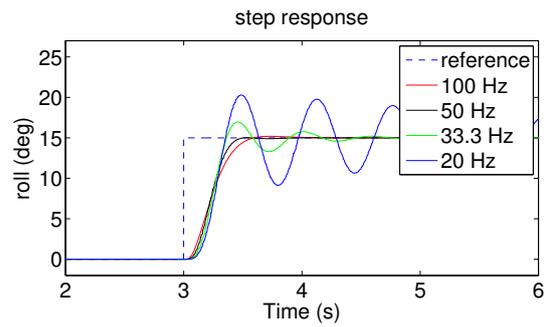
Figure 10: Sampling frequency sensitivity test.

As the designed controller only concerns the quadrotor attitude stabilization, we will only consider the disturbances in terms of torques, which are described by

$$\boldsymbol{\tau}_D = \mathbf{D}_r \boldsymbol{\omega}_a^2 \qquad (39)$$

where D_r is a rotational drag coefficient matrix and $\boldsymbol{\omega}_a$ is the true air relative angular rate.

The tests concern the quadrotor response to constant wind steps of different values, namely the controller actuation torque request and respective attitude.

In figure 11 we present the INDI obtained, namely the torque request in 11(a) and the quadrotor roll angle in 11(b). The INDI controller shows a quick but small torque to counteract the wind disturbance. As a result of this torque, we can observe the roll angle increasing in the first 0.2 seconds, followed by a decrease and stabilization at 0 degrees before the mark of 0.8 seconds, demonstrating the expected disturbance rejection of this solution.

After the system stabilizes we apply a step of 15 degrees to the roll reference so we can observe if the quadrotor maneuvers correctly under the wind disturbance.

Figure 12 shows the INDI control action request (fig. 12(a)) to the roll reference step, and respective response (fig. 12(b)). The control action shows a small variation for different wind intensities, guaranteeing the insensitivity of the roll response to the increase of the wind intensity.

7 CONCLUSIONS

This paper presents the incremental version of the nonlinear dynamics inversion control approach, and applies it to the quadrotor attitude control problem. The theoretical formulation of INDI is presented alongside with the NDI formulation for a better comparison of approaches. The same is done when the INDI formulation is applied to the specific case of

(a) Torque τ_x request
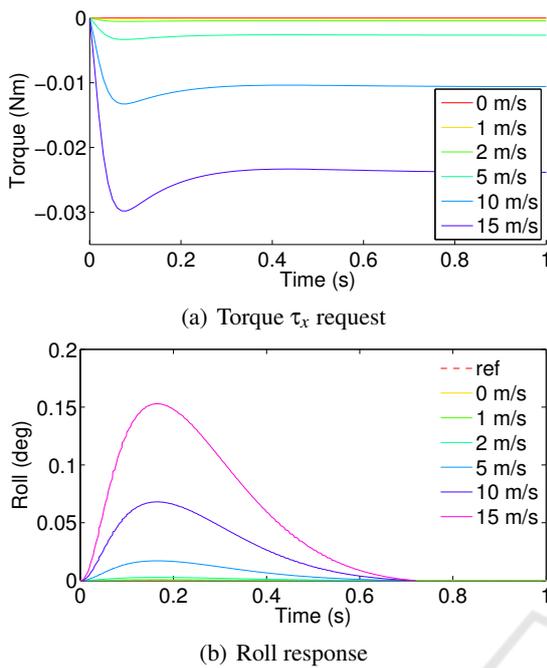
(b) Roll response

Figure 11: INDI response to constant wind disturbance.

(a) Torque τ_x request
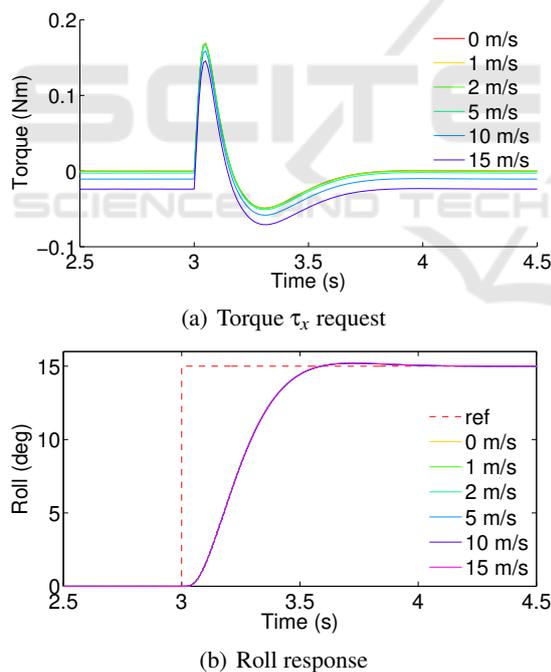
(b) Roll response

Figure 12: INDI response to roll step reference with constant wind disturbance.

the quadrotor attitude control. This is done after the quadrotor model is presented, and it allows us to better acknowledge the specificities of the approaches. While NDI is a model-based approach, dependent on an accurate system model, the INDI solution substitutes this model knowledge requirement by accurate

sensor measurements and/or variables estimation, and high enough sampling times.

For an easier and more straightforward INDI control design, this paper addresses implementation issues like INDI parameter tuning, linear control design and angular acceleration estimation. INDI is an intrinsically integrative control approach, where the present control action is obtained varying the previously applied control action. We show that this variation should be weighted similarly to an integrative term in PID control, and demonstrate this by simulating the closed-loop response for different weights.

We demonstrate the INDI robustness to model uncertainties varying the quadrotor inertia. We show that, in this case, the INDI approach handles an inertia estimation variation between 0.5 and 1.5 times the true value, considering real sensors and estimators. An underlying assumption in INDI is that the controller sampling rate is higher than the system higher frequency in order to neglect states variation between samples. A sensitivity analysis to the controller sampling frequency is also done, showing that the INDI performance is indeed compromised by this parameter choice. However, given the processing capabilities of today's processors, the bottleneck for this choice lies not in the processor capacities but rather on the acquisition rates of the existing sensors set.

Finally, results demonstrate the robustness of the solution in the presence of wind disturbances. The INDI controller not only is able to reject the disturbance but is also able to properly follow attitude references even with increased wind intensity.

ACKNOWLEDGEMENTS

REFERENCES

Azinheira, J., Moutinho, A., and Carvalho, J. (2015). Lateral control of airship with uncertain dynamics using incremental nonlinear dynamics inversion. *IFAC-PapersOnLine*, 48(19):69–74.

Bastin, G. (2013). *On-line estimation and adaptive control of bioreactors*, volume 1. Elsevier.

Esteves, D., Moutinho, A., and Azinheira, J. (2015). Stabilization and altitude control of an indoor low-cost quadrotor: design and experimental results. In *Proc. 2015 IEEE International Conference on Autonomous Robot Systems and Competitions*, pages 150–155, Vila Real, Portugal. IEEE.

Goman, M. and Kolesnikov, E. (1998). Robust nonlinear dynamic inversion method for an aircraft motion control. *AIAA Paper*, pages 98–4208.

Krstic, M., Kokotovic, P. V., and Kanellakopoulos, I. (1995). *Nonlinear and adaptive control design*. John Wiley & Sons, Inc.

Liao, F., Wang, J. L., and Yang, G.-H. (2002). Reliable robust flight tracking control: an lmi approach. *Control Systems Technology, IEEE Transactions on*, 10(1):76–89.

Mallikarjunan, S. and et al. (2012). L1 adaptive controller for attitude control of multirotors. In *AIAA Guidance, Navigation, and Control Conference*, pages 1–15, Minnesota, USA. AIAA.

Sadeghzadeh, I., Mehta, A., and Zhang, Y. (2011). Fault/damage tolerant control of a quadrotor helicopter UAV using model reference adaptive control and gain-scheduled PID. In *AIAA Guidance, Navigation, and Control Conference*, pages 1–13, Oregon, USA. AIAA.

Sieberling, S., Chu, Q., and Mulder, J. (2010). Robust flight control using incremental nonlinear dynamic inversion and angular acceleration prediction. *Journal of guidance, control, and dynamics*, 33(6):1732–1742.

Simplício, P., Pavel, M., Van Kampen, E., and Chu, Q. (2013). An acceleration measurements-based approach for helicopter nonlinear flight control using incremental nonlinear dynamic inversion. *Control Engineering Practice*, 21(8):1065–1077.

Stevens, B. and Lewis, F. (2003). *Aircraft control and simulation*. John Wiley & Sons.